Results in Engineering 29 (2026) 109291

Contents lists available at ScienceDirect

Results in Engineering

journal homepage: www.sciencedirect.com/journal/results-in-engineering

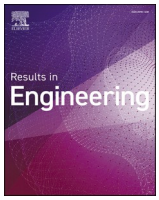

Effectiveness of *Phoenix* sp. particles as reinforcement in epoxy composites: Mechanical, free vibration, thermal, and water absorption characteristics

G. Rajeshkumar [a,*], A. Poovarasan [a], S.V. Naren Prasaadh [a], M.R. Sanjay [b], Suchart Siengchin [b]

[a] Department of Mechanical Engineering, PSG Institute of Technology and Applied Research, Coimbatore, Tamil Nadu, India
[b] Natural Composites Research Group Lab, Department of Materials and Production Engineering, The Sirindhorn International Thai-German Graduate School of Engineering (TGGS), King Mongkut's University of Technology North Bangkok (KMUTNB), Bangkok, Thailand

ARTICLE INFO

Keywords:
Natural filler
Epoxy
Mechanical properties
Free vibration
Thermal stability

ABSTRACT

Integrating natural fillers into polymer composites has been identified as a feasible and viable technique for improving performance of the material with preserving sustainability. In this work epoxy-based composites are fabricated by incorporating *Phoenix sp.* natural fillers in different weight proportions using compression moulding process and subjected to various experimental testings. The findings indicated that, the composites containing 10 wt.% of filler shows highest tensile, flexural and impact strengths, and vibration characteristics of 26 MPa, 47.6 MPa, 10.5 kJ/m^2, and 24.16 Hz, respectively. In addition, morphological analysis of the mechanically tested samples provided insights into effective interfacial bonding. The thermal degradation analysis showed higher stability at 15 wt.% filler content, with reduced weight loss (75.43%) during the main degradation phase (stage-3) and the highest degradation temperature observed in the DTG curve is 391.9 °C. The hydrophilic property was noted in the water diffusion process, where an increase in filler content affects the water uptake rate of the composites. The *Phoenix* sp. filler added epoxy composites with increased mechanical, thermal and vibration characteristics could be employed in engineering applications such as roofing panels, insulation covers, and automotive and machine tool industries.

1. Introduction

The growing awareness on environmental concerns including air and water contamination, rising carbon footprints, and stacking up in landfills has encouraged the development and adoption of sustainable alternatives to conventional materials. The initiatives in promoting biodegradable and renewable-resource-based materials are part of a greater global movement for environmentally friendly practices in science, engineering, and technology is highly required [1,2]. This trend aligns with environmental conservation and sustainable development initiatives, which highlight the importance of reducing humankind's ecological imprint while ethically fostering technological progress [3]. These concepts are being adopted by governments and businesses worldwide in an attempt to strike a balance between preserving natural resources for future generations and promoting economic growth. Additionally, using renewable resources reduces reliance on petroleum products, which negatively affects the environment through greenhouse gas, increases the necessity in the production of distinctive bio-based products [4,5]. This shift positively impacts environmental restoration by lowering atmospheric carbon dioxide levels. Recent research has focused on integrating advanced decision-making frameworks to select materials based on both performance and environmental impact. This shift toward eco-friendly materials spans a wide range of categories and types, extending to diverse applications such as construction, packaging, textiles, and energy solutions [6–8]. Adoption of these materials promotes waste reduction, resource conservation, and the transition to a more sustainable future [9]. Many of such materials have high strength-to-weight ratios, which enhance a material's performance for a variety of applications, in addition to addressing concerns like biodegradability and dependability [10,11].

Polymer composites are popular due to their low density, high specific strength and stiffness, ease of manufacturing, and cost effectiveness. Natural fillers have recently been considered as a viable reinforcement in polymer composites due to their lightweight, biodegradable nature and other functional features equivalent to their synthetic counterparts [12–14]. In particular, the plant-derived fillers have

* Corresponding author.
E-mail address: grajeshkumar.me@gmail.com (G. Rajeshkumar).

https://doi.org/10.1016/j.rineng.2026.109291
Received 1 July 2025; Received in revised form 5 December 2025; Accepted 26 January 2026
Available online 26 January 2026

gained increasing attention due to their renewable origin, low cost, and wide availability, particularly in regions where these plants grow abundantly. Despite of their properties such as bio degradability and low density, they also possess high surface area, which helps to improve the bonding between matrix and reinforcement [15,16]. Therefore, researchers have increasingly focused on the use of plant-based natural particles as fillers in polymer composites [17]. Nagaprasad et al. [18] investigated the impact of date palm seed filler loading on mechanical and thermal properties of vinyl ester-based composites, highlighting the suitability of natural particles in vinyl ester composites. The results disclosed that, the composites added with 30 wt. % of filler significantly enhanced the mechanical and thermal properties. Based on the outcomes, the optimized composites were recommended for various applications, including automotive components and home appliances such as table fan blades, self-motor guards for heavy load vehicles, and engine guards for two-wheelers. Similarly, Nagarajan et al. [19] evaluated the mechanical and thermal behaviour of polymeric composites reinforced with agro waste α-cellulosic micro filler. Experimental data revealed that the composites loaded with 15 wt. % exhibited superior mechanical and thermal properties. This enhancement is attributed to improved filler dispersion and strong adhesion between the matrix and α-cellulosic microfiller, which facilitates more effective stress transfer. Recently automotive industries are replacing their synthetic material with bio-based composite, which include natural fillers as their major reinforcement due to the stringent environmental regulations. Applications of natural filler reinforced polymer composites also includes aerospace, defence, construction and electronic applications were keep on evolving [20].

Phoenix sp. plants belong to the *Arecaceae* family and *Coryphoideae* sub family, they are majorly found in Africa, China, Turkey, Canary Islands, and India [21]. This plant's fruit is extremely small, with a wide opening seed protected by a thin layer of pulp, and it is barely consumed by humans. Furthermore, these plants contain 15 to 25 petioles and are majorly used for decoration purposes. Previous studies have employed fibers isolated from petioles as reinforcement in polymer composites and have reported considerable improvements in their properties [22,23]. In the context of turning waste into useful materials, the petioles can be processed into fillers for polymer reinforcement, which may help to improve certain material properties, reduce the cost, and broaden their potential applications.

This work aims to produce environmentally friendly composites with considerable performance by incorporating *Phoenix* sp. petiole fillers (PPF) into an epoxy matrix. The properties such as tensile, flexural, impact, hardness, thermal stability, free vibration and moisture absorption characteristics were explored interms of PPF content. Furthermore, the surface morphology and the fracture mechanism of *Phoenix sp*. petiole filler Reinforced Epoxy Composite (PPFEC) were examined using Scanning Electron Microscope (SEM). The outcome of this study indicate that the resulting composite exhibits a favourable balance on weight and mechanical performance. The findings suggest that this material may be suitable for applications where lightweight composites are required.

2. Materials and methods

2.1. Material

The *Phoenix* sp. petioles were obtained from in and around the Coimbatore region, Tamil Nadu, India. The lengthy stalks were cut into smaller pieces and dried in sun light for about 15 days. The stalks are then ground into a fine powder, which is subsequently passed through a sieve (100 μm) shaker to eliminate any uneven particulates (Fig. 1). For

Fig. 1. Preparation steps of PPF and PPFEC.

fabricating composites, epoxy resin (LY556) and hardener (HY951) procured from M/s Covai Seenu & Co., Coimbatore, India, were employed as the matrix material and their characteristics are detailed in the Table 1.

2.2. Fabrication of composite

The composite lamina was prepared by incorporating different wt. % of PPF (5, 10, 15, and 20 wt. %) into epoxy matrix through compression moulding method. The mixture was prepared by adding the PPF to the resin and stirred using a mechanical stirrer for about 5 min to obtain even distribution of PPF throughout the resin. The mixture is then poured into the prepared mold having size of 300 mm x 300 mm x 3 mm. To enable easy removal of the lamina, the silicone spray was applied on all surfaces of the mold. The mixture was allowed to cure for about 8 h under a constant load of 100 N to ensure uniform thickness (Fig. 1). The specimens are subsequently cut using a CNC machine in accordance with ASTM standards and stored in an airtight container until testing.

2.3. X-Ray diffraction (XRD)

XRD is a widely used analytical technique for characterizing the material'scrystalline structure. It provides detailed information about a material's crystalline structure, which is considered as important aspects in understanding their performance when reinforced into a polymer for composite applications. Additionally, the crystallinity index (CI) was calculated applying the Eq. (1).

$$CI\ (\%) = \frac{I_{200} - I_{amp}}{I_{200}} \times 100 \tag{1}$$

where, I_{200} denotes maximum intensity of the crystalline peak, and I_{amp} corresponds to intensity of the amorphous background.

2.4. FTIR

FTIR spectroscopy is an analytical technique for the detection of functional groups and determining the composition of materials. The SHIMADZU FTIR Spectrophotometer was employed in the investigation. The spectrum is documented in the wavenumber range of 400 – 4000 cm^{-1}. Furthermore, the FTIR spectrum is recorded at a resolution of 4 cm^{-1}, with 45 scans averaged to achieve an optimal signal-to-noise ratio.

2.5. Morphological analysis

The morphological analysis of the particle as well as fractured samples was accomplished using an FESEM (CARL ZEISS, USA) with a resolution of 1.5 nm, and an accelerating voltage of 12 kV. To enhance conductivity, the specimens were gold-coated before imaging.

2.6. Mechanical testings

A universal testing machine (INSTRON 8801) with a capacity of 100 kN was used to test the tensile properties of the composites. In adherence to ASTM D638 standard, the samples were prepared with dimensions of 167 mm × 12 mm × 3 mm. The same machine, operating at a crosshead speed of 2.5 mm/min was used to test the flexural properties of the prepared samples with dimensions of 125 mm × 12.7 mm × 3 mm as per ASTM D790 standard. The impact test was conducted using an Izod impact testing machine (Deepak Poly Plast Pvt. Ltd, India) equipped with a pendulum possessing a potential energy of 2.57 J. Test specimens were made with specifications of 64 mm × 12.7 mm × 3 mm in line with ASTM D256. Using a digital Shore D durometer with a range of 0–100 HD, a resolution of 0.5 HD, an indenter depth of 0–2.5 mm, and a test pressure of 0–45.5 N, the hardness of the fabricated sample was measured. The samples were firmly positioned on a slab, and the indenter needle was applied vertically to measure the hardness value. Five specimens from each variation were used for all the above tests, and their average value was recorded.

Table 1
Characteristics of LY556 - Epoxy resin.

S. No.	Test	Test method	Specification	Unit
1.	Aspect	Visual	Clear-pale, yellow liquid.	–
2.	Color	Hardner, ISO:4630	≤ 2	–
3.	Epoxy content	ISO: 3000	5.30–5.45	eq/kg
4.	Viscosity at 25 °C	ISO: 12,058–1	10,000 – 12,000	mPa/s
5.	Density at 25 °C	ISO: 1675	1.15 – 12.0	g/cm
6.	Flash point	ISO: 2719	>200	°C

2.7. Numerical analysis

The tensile modulus of the PPFECs was theoretically estimated using a micromechanical model based on the Halpin-Tsai approach. This model has been chosen for natural filler composites owing to its simplicity and applicability, regardless of the existence of various theoretical prediction models. The composite was assumed to be isotropic, homogeneous, and linearly elastic in behaviour. The Eqs. (2)-(4) were used to determine the modulus values [24,25].

$$V_f = \frac{w_f/\rho_f}{(w_f/\rho_f) + ((1 - w_f)/\rho_m)} \tag{2}$$

$$\eta = \frac{E_f - E_m}{E_f + \xi E_m} \tag{3}$$

$$E = E_m\left(\frac{1 + \xi\eta V_f}{1 - \eta V_f}\right) \tag{4}$$

where E_f and E_m are the Young's modulus of filler and matrix material, respectively. V_f and V_m are volume fractions of filler and matrix material, respectively. ρ_f and ρ_m denotes the density of filler and matrix, respectively. ξ is an arbitrary variable, also called an empirical factor, considered based on the assumptions. It depends on particle geometry; therefore, several values were evaluated (ξ = 0, 1, 2), and the final comparison was made using the value that best matched the experimental trend.

2.8. Vibration test

Free vibration tests were performed using the experimental setup imported from Hottinger Brüel & Kjaer, Denmark, to determine the natural frequency of the specimen having size of 250 mm x 25 mm x 3 mm. For conducting the test, a triaxial accelerometer (10 mV/g) was fixed at the free end of the specimen and the other end was fixed using a clamp to make cantilever arrangement. An initial force was applied on the specimen using the impact hammer (22.7 mV/N) at several points and the obtained data was analysed by Fourier transform. The readings were obtained from five distinct points of the composite and their average is reported as the natural frequency of the specimen.

2.9. Thermogravimetric analysis (TGA)

The TGA was performed using a PerkinElmer, TGA 4000 analyzer under a nitrogen atmosphere to assess the thermal stability of the sample. A sample of 5 mg were heated at a rate of 20 °C/min up to a temperature of 900 °C and the weight loss was recorded. For each sample, the test was performed twice to confirm the consistency of the results.

2.10. Differential scanning calorimetry (DSC)

The thermal properties of the prepared samples were studied using PerkinElmer, DSC 6000 with the heating rate of 10 °C/min from ambient conditions to 400 °C. The test samples of 2 mg were placed in an alumina crucible and the temperature was varied under nitrogen atmosphere. The test was conducted twice for every sample to verify the consistency of the measurements. Finally, the DSC curves were plotted using the obtained data.

2.11. Water absorption test

In accordance with ASTM D570, the test pieces were cut with a size of 64 mm x 12.7 mm x 3 mm and soaked in distilled water at ambient temperature to evaluate their water absorption capacity. At periodic intervals, the sample's weight was measured and using the samples initial and final weights the moisture absorption percentage was computed.

2.12. Water contact angle

The water contact angle that reflects the wettability of the samples was measured using a Kyowa Goniometer. A droplet of deionized water was gently placed on the surface, and its image was captured with a camera. The contact angle was then calculated through image analysis software.

3. Result and discussion

3.1. XRD analysis

The structural characteristics of PPF were analyzed to ascertain their crystallinity, a crucial factor in comprehending their performance when incorporated into a polymer for composite applications. The diffraction pattern of PPF depicted in Fig. 2 exhibited two peaks at $2\theta = 16.3^{\circ}$ and $2\theta = 22.6^{\circ}$ Notably, the peak at $2\theta = 22.6^{\circ}$ corresponds to the (200) crystallographic plane, indicating an organised cellulose structure in natural biomass particles [26]. Furthermore, the CI of PPF was found to be 60.97 %, indicating a moderate degree of crystallinity. This reflects a balance between ordered and disordered regions, suggesting a semi-crystalline structure of the particles. This semi-crystalline structure is essential for determining the compatibility of the fillers with polymer matrices, as well as its ability to influence the composite's mechanical and thermal properties.

3.2. FTIR

The functional groups that exist in the PPF (Table 2) holds an ability to affect the overall properties of the PPFEC. The FTIR curve and the

Table 2
Functional groups present in PPF.

Wavenumber (cm^{-1})	Functional Group	Type of Vibration (Stretching/Bending)	References
3357	–OH (Hydroxyl)	O–H Stretching (Broad)	[30]
2925	–CH (Aliphatic C–H)	C–H Stretching (Asymmetric)	[28]
2364	–C≡C (Alkyne)	C≡C Stretching	[30]
1611	*C = C* (Aromatic or Alkene)	*C = C* Stretching (Conjugated)	[30]
1369	–CH_3 (Methyl)	C–H Bending (Symmetric)	[30]
1103	C–O (Ether or Ester)	C–O Stretching	[31]
1035	C–O (Carbohydrate/ Alcohol)	C–O Stretching	[30]
860	Aromatic C–H	C–H Bending	[28]

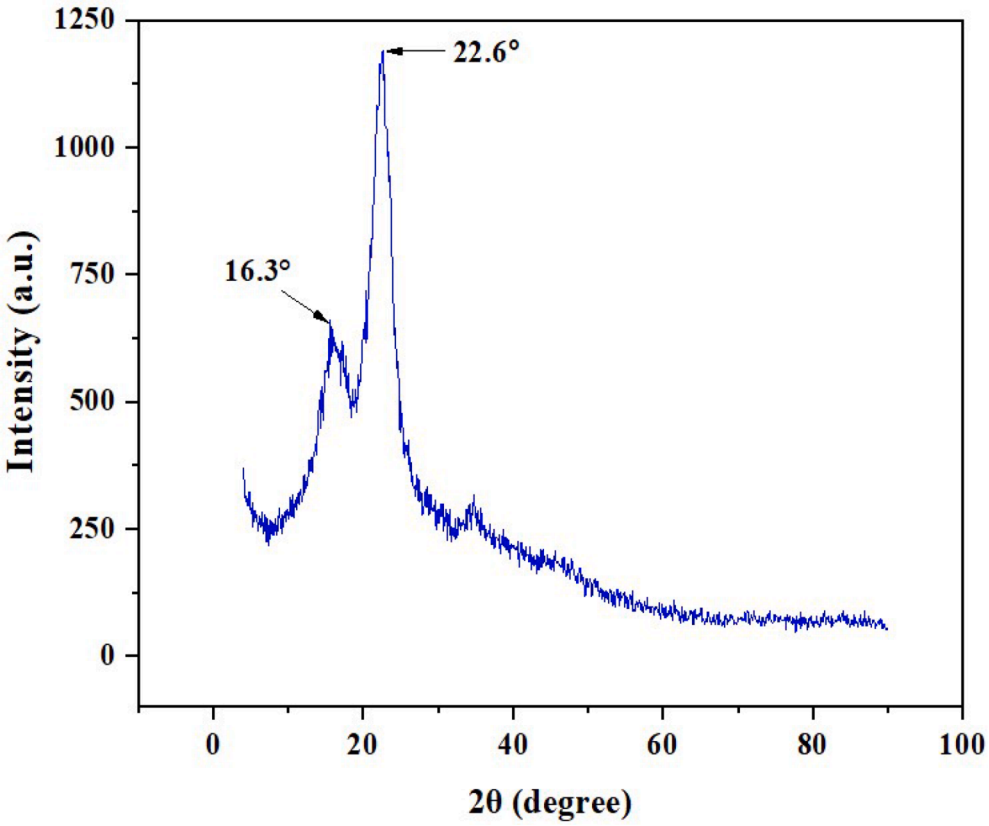

Fig. 2. XRD pattern of PPF.

obtained peaks are displayed in Fig. 3. The O-H (hydroxyl) group in cellulose, hemicellulose, and lignin enhances hydrophilicity and hydrogen bonding, resulting in improved polymer-matrix interaction [27]. However, it promotes moisture absorption, which might reduce mechanical and thermal durability of the composites. The C-H (aliphatic C-H) group commonly present in the primary constituents of biomass such as lipids, lignin, and hemicellulose reflects the organic content of PPF which influences the thermal stability of resulting composites [28]. Furthermore, the aliphatic structures degrade at a lower temperature than aromatic structures. The C≡C groups, which are less prominent, may arise from lignin or protein changes which affects the chemical reactivity [29]. The presence of these functional groups determines thermal stability, hydrophilicity, and interfacial adhesion in polymer composites, necessitating proper biomass treatments to maximise the performance.

3.3. Morphological analysis

The SEM images (Fig. 4a) show the uneven, rough surface of the PPF with uneven edges, suggesting its irregular appearance, which improves interfacial adhesion when added to a polymer matrix. The increased surface roughness improves mechanical interlocking, allowing for greater stress transmission between the matrix and the filler, potentially leading to improved mechanical characteristics [32]. The particle shape is noted to be a combination of angular and elongated structures which improve mechanical support by enhancing load bearing capability by developing the aspect ratio. In addition, the size range of the particles is crucial which affects the dispersion ability of the filler within the polymer matrix [33]. The particle size distribution graph (Fig. 4b) assists in characterising the filler, by displaying a histogram with a Gaussian fit which demonstrates a normal distribution of particle sizes. The graph indicates that, the majority of the particles fall within the 42 μm size range, with minimal size deviation. A controlled particle size distribution ensures, homogeneous stress distribution that lowers the possibility of presence of weak regions in the composites.

The chemical composition of PPF particles was analyzed using Energy Dispersive X-ray Analysis (EDAX), which revealed a major presence of carbon (56.99 %) and oxygen (40.86 %), along with minor amounts of silicon (0.17 %), chlorine (0.83 %), potassium (0.82 %), calcium (0.14 %) and magnesium (0.19 %) (Fig. 4c). The high carbon content indicates the organic nature of the filler, enhancing its compatibility with polymer matrices and improving mechanical strength [34]. The presence of silicon and calcium indicates thermal stability and stiffness of the PPF, whereas magnesium and potassium involve in promoting the interfacial adhesion between polymer and reinforcement, resulting in effective stress transmission. These characteristics make PPF a promising natural filler for enhancing the mechanical strength and thermal stability of polymer composites while promoting sustainability.

3.4. Mechanical properties

The tensile characteristics of PPFEC specimens is presented in the Fig. 5a, revealing the influence of filler content on tensile strength (TS) and tensile modulus (TM). The TS and TM of neat epoxy is noted to be 22.02 MPa and 1.7 GPa, respectively. Incorporating PPF particles to the composite increases both the TS and TM of the composite compared to neat epoxy, demonstrating the effect of particle reinforcement on tensile properties. This enhancement is due to the high aspect ratio of PPF,

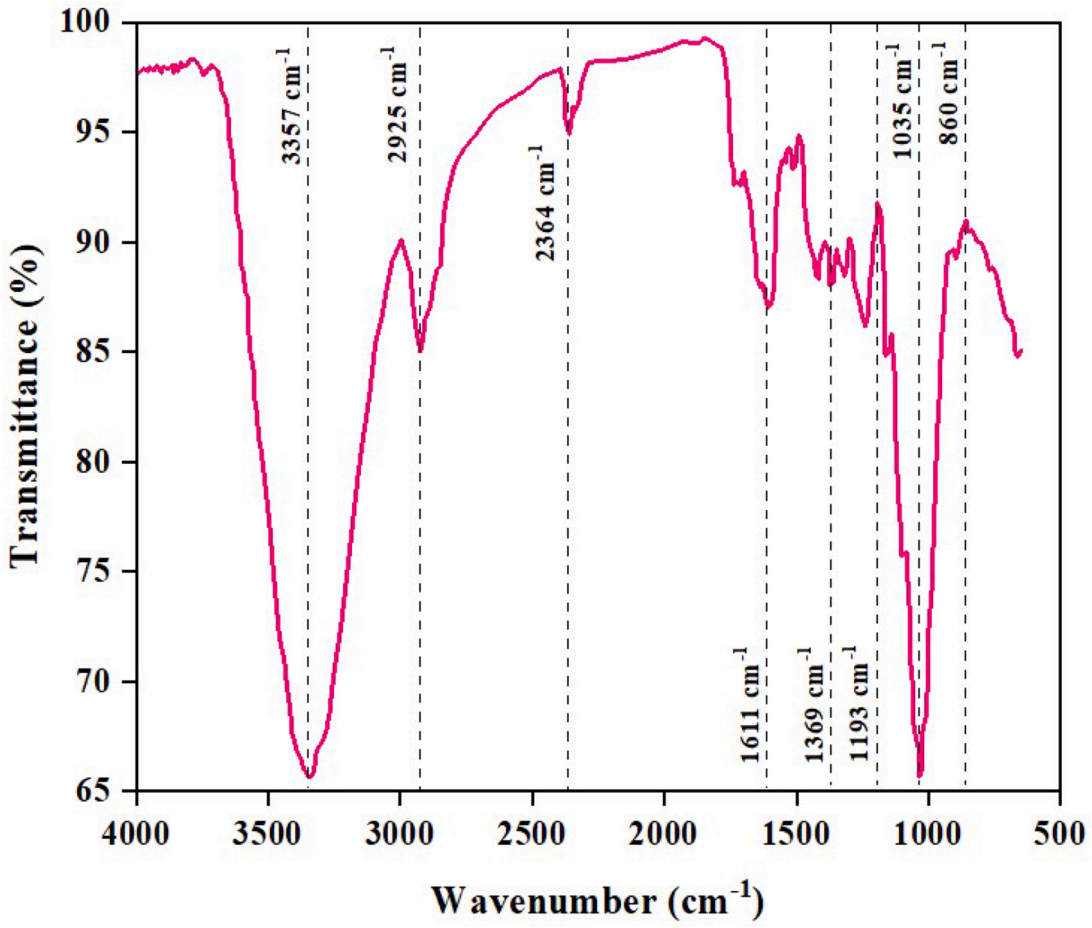

Fig. 3. FTIR curve of PPF.

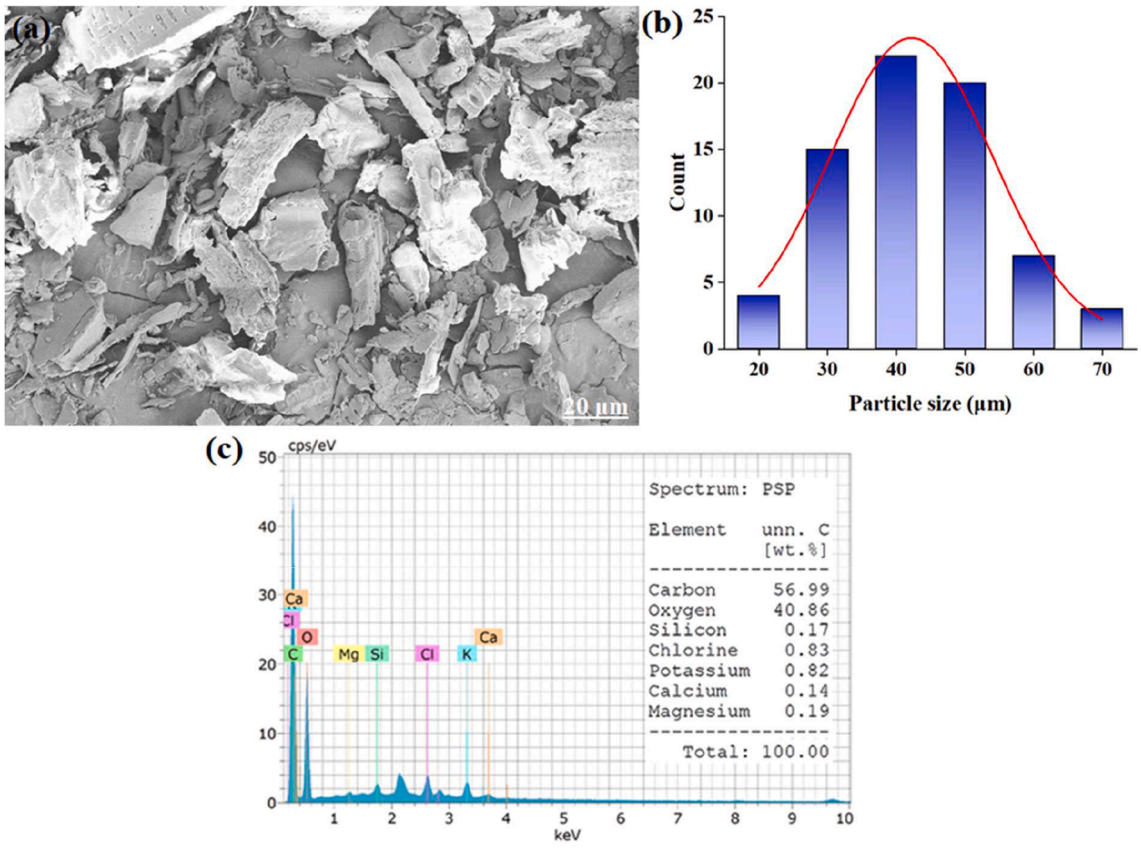

Fig. 4. Particle size analysis: (a) SEM, (b) particle size distribution, and (c) elemental composition (EDS analysis) of PPF.

which facilitate efficient stress distribution at the interface [35]. As the concentration of the particle increases the TS and TM also following a rising trend. Especially, the TS and TM reaches its peak value of 31.08 MPa and 3.52 GPa, respectively when 10 wt. % of the PPF is reinforced in to the epoxy. This enhancement is mostly attributed to strong resin-particle interfacial adhesion. However, increasing the PPF content beyond 10 wt. % reduces the TS and TM due to the increased void content and filler agglomeration, leading to poor dispersion and weak interfacial bonding between the filler and the matrix. Additionally, an imbalance in the filler-to-matrix ratio creates particle blockage, hindering stress transfer and contributing to premature fracture and composite failure [36].

Fig. 5b shows the flexural strength (FS) and flexural modulus (FM) of the PPFEC samples. It is evident that, the addition of PPF increase the FS (44.82 MPa) and FM (1.92 GPa) of neat epoxy, highlighting the critical impact that particle reinforcement plays in enhancing stiffness, interfacial bonding, and stress transfer between the matrix and filler [35]. As the filler loading increases, both FS and FM improve significantly, reaching their peak values at 10 wt. % reinforcement (i.e. highest FS and FM of 53.31 MPa and 3.09 GPa, respectively). This enhancement is credited to the strong adhesion and better interfacial adhesion between the particle and the matrix. The flexural characteristics starts to deteriorate as the filler content increases above this limit since the particles start to accumulate at some regions in the composites, decreasing the filler-matrix adhesion and causing cracks and decreased bending stress in the composite [37,38].

The impact characteristics of the PPFEC interms of PPF content is illustrated in the Fig. 5c. It is noticed that, the neat epoxy exhibits a relatively low impact strength (IS) of 4.83 kJ/m^2, indicating that the unreinforced polymer lacks the ability to withstand applied impact loads, resulting in limited energy absorption. As the reinforcement quantity increases, the IS also improves, which can be ascribed to the high modulus of the particles that enhance the toughness of the composite. The composites incorporated with 10 wt. % of PPF recorded the maximum IS of 9.92 kJ/m^2, which is 105.38 % greater than the neat epoxy. When the filler content is further increased (i.e. 15 wt. % and 20 wt. %), it produces a contrast effect with a reduction in IS. This could be due to the formation of clusters that introduce the agglomeration effect where the fillers restrict the even distribution throughout the matrix. This phenomenon involves the occurrence of stress concentration, which induces the propagation of a crack and finally attains the failure of the composite [39].

Fig. 5d depicts the hardness of the PPFEC with respect to the variations in filler content. The neat epoxy composite exhibits hardness of 64. When reinforced with PPF, the composite's Shore D hardness increase compared to the pure epoxy composite. It is evident that, the hardness of the neat epoxy increases after the inclusion of PPF. This is because, the addition of PPF resist deformation under applied stress, as a result of better bonding among the filler and matrix [40]. Furthermore, the hardness of PPFEC increases proportional to the increase in particle content. Especially, when the composite is loaded with 10 wt. % of PPF, the hardness reaches to a value of 83, which is due to the strong adhesion between the composite parts, that enhances the composite's stiffness. In addition, this value is 29.68 % greater than the neat epoxy. Contrarily, when the reinforcement exceeds 10 wt. %, the hardness of the composite tends to decrease due to a weakened interfacial bond between the matrix and PPF, which compromises the structural integrity and reduces the composite's durability under external loads [41].

Table 3 presents a comparative analysis of the mechanical properties of the present study with other natural filler reinforced composites. The results indicate that PPFEC exhibits tensile and flexural strengths that are comparable to those reported for similar natural filler–based composites. Notably, the hardness of PPFEC is significantly higher than that of the other composites considered, highlighting its superior resistance

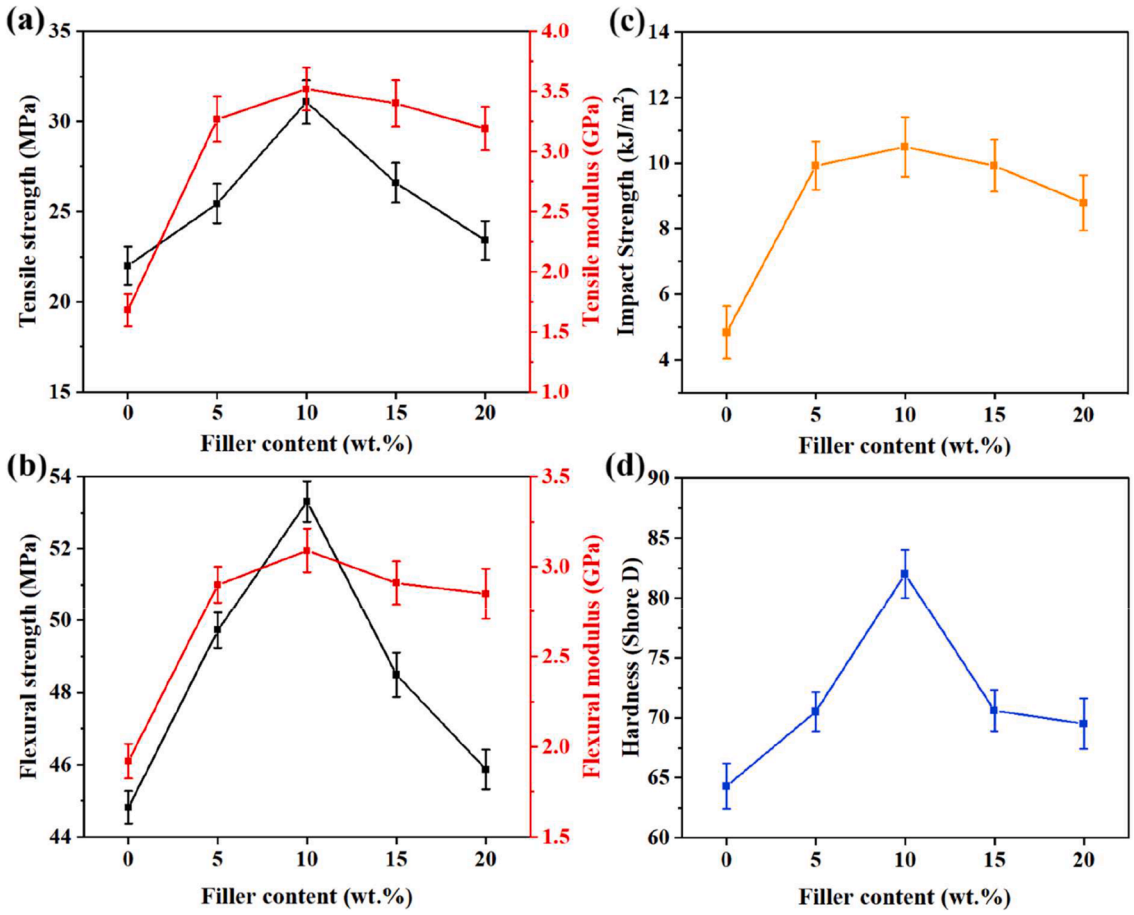

Fig. 5. Mechanical characteristics: (a) tensile, (b) flexural, (c) impact, and (d) hardness properties of PPFEC.

Table 3
Comparison of mechanical properties of different natural filler added composites.

Filler	Matrix	Manufacturing Method	Loading wt. %	Tensile Strength (MPa)	Tensile Modulus (GPa)	Flexural Strength (MPa)	Flexural Modulus (GPa)	Hardness	Impact Properties (kJ/m^2)	Reference
Phoenix sp.	Epoxy	Compression moulding	10	31.08	3.52	53.31	3.09	82	10.5	Present work
Elaeocarpus ganitrus seeds	Epoxy	Hand lay-up	10	42.30	0.91	87.4	5.5	-	-	[42]
Wood apple shell	Epoxy	Hand lay-up	15	45.6	-	78.19	-	-	-	[43]
Ipomoea carnea	Epoxy	Hand lay-up	30	23.75	7.2	52.47	4.38	23.1	9	[44]
Tamarind seed	Polypropylene	Melt mixing	30	20.6	-	-	-	-	-	[45]
Orange peel	Epoxy	Hand lay-up	20	5.85	-	62.35	-	20.72	-	[46]
Tamarind seed	Vinyl ester	Compression moulding	15	34.1	2.05	121	-	42.33	14.02	[47]
Polyalthia longifolia seed	Vinyl ester	Compression moulding	25	32.50	1.23	125	-	36.5	31.09	[48]
Date palm seed	Vinyl ester	Compression moulding	30	40.3	-	149	-	51.08	17.03	[18]
Tea dust	Epoxy	Hand lay-up	40	14	1.442	39	2.17	-	0.625	[49]

to indentation.

The results clearly indicate that the mechanical properties are influenced by the filler content, which served as the sole independent variable in this study. Since the filler content included five levels, a one-way ANOVA was conducted for all the mechanical properties, and the corresponding outcomes are presented in the Table 4. It is evident that the p-values for all the mechanical properties are <0.05, confirming that the filler content has a statistically significant effect on the mechanical performance of the composites. Notably, the flexural strength exhibits the lowest p-value of 0.018104, indicating that it is the most strongly influenced by changes in filler content. On the other hand, all the computed F-value was higher than the F-critical value, the null hypothesis of equal group means was rejected, demonstrating that the factor under study (filler content) has a significant influence on the response variable (mechanical properties).

3.5. Comparison between theoretical and experimental modulus values

The comparison of Halpin-Tsai model predictions and experimental tensile modulus of the composites with different filler contents is

Table 4
ANOVA results for the mechanical properties.

Tensile strength						
Source of Variation	Sum of Squares	df	Mean Square	F	p-value	Fcrit
Between Groups	85.23873	3	28.41291	4.502175	0.024538	3.490295
Within Groups	75.73116	12	6.31093	-	-	-
Total	160.96989	15	-	-	-	-
Tensile modulus						
Source of Variation	Sum of Squares	df	Mean Square	F	p-value	Fcrit
Between Groups	2.081875	3	0.693958	4.331599	0.027516	3.490294
Within Groups	1.9225	12	0.160208	-	-	-
Total	4.004375	15	-	-	-	-
Flexural strength						
Source of Variation	Sum of Squares	df	Mean Square	F	p-value	Fcrit
Between Groups	86.72846	3	28.90948	4.970281	0.018104	3.490294
Within Groups	69.79762	12	5.81646	-	-	-
Total	156.52609	15	-	-	-	-
Flexural modulus						
Source of Variation	Sum of Squares	df	Mean Square	F	p-value	Fcrit
Between Groups	2.66	3	0.886667	4.172549	0.030676	3.490294
Within Groups	2.55	12	0.2125	-	-	-
Total	4.004375	15	-	-	-	-
Impact strength						
Source of Variation	Sum of Squares	df	Mean Square	F	p-value	Fcrit
Between Groups	3.4402	3	1.146733	3.71933618	0.042260	3.490294
Within Groups	3.6998	12	0.308316667	-	-	-
Total	7.14	15	-	-	-	-
Hardness						
Source of Variation	Sum of Squares	df	Mean Square	F	p-value	Fcrit
Between Groups	319.37	3	106.45667	4.10006	0.032256	3.490294
Within Groups	311.58	12	25.965			
Total	4.004378	15	-	-	-	-

illustrated in Fig. 6. The theoretical model predicts an upward trend in modulus with increasing filler content as the particles restrict the deformation of the polymer and improve the stiffness of the material. In line with the theoretical predictions, the experimental results follow the similar increasing trend up to 10 wt. % filler, exhibiting the maximum tensile modulus with the value of 3.52 GPa. Beyond this loading, a reduction in modulus is observed. This deviation from the theoretical curve is expected because the Halpin–Tsai model assumes ideal

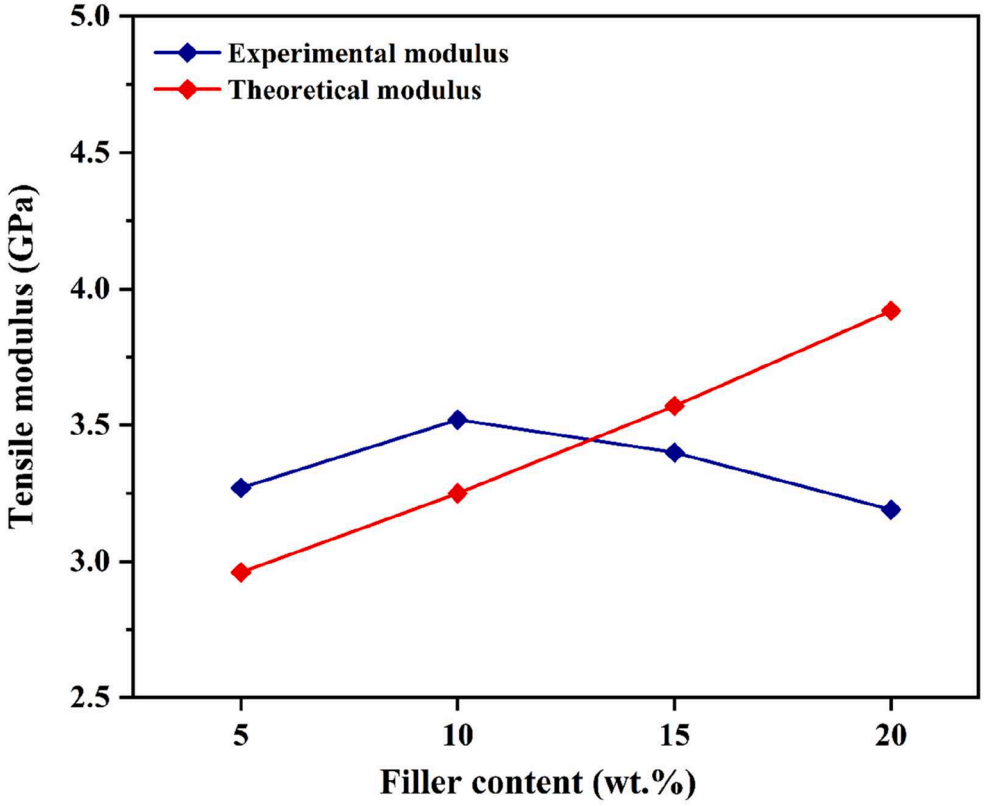

Fig. 6. Theoretical and experimental elastic modulus of PPFEC.

dispersion and perfect particle–matrix bonding. At high filler loadings, the agglomeration of particles arises within the matrix, causing poor interfacial bonding between composite elements. These factors reduce effective stress transfer and lower stiffness, leading to negating the modulus that the Halpin–Tsai model does not capture. As a result, the micromechanical model acts as a baseline prediction, although the differences at higher filler levels underline the effect of real microstructural effects.

3.6. Free vibration

The free vibration characteristics of PPF reinforced epoxy composites were investigated to evaluate their natural frequency. Fig. 7 illustrates the fundamental natural frequency (NFY) of the PPFEC in accordance with filler content. The NFY of the composites enhances with the addition of filler into the epoxy matrix. It is observed that the neat epoxy exhibits an NFY of 17.09 Hz and reaches to a maximum value of 24.16 Hz when 10 wt. % of PPF is reinforced in to the epoxy. This enhancement is attributed to the strong interfacial bonding of composite elements, which makes the composites stiffer than the matrix. Moreover, improved mechanical attributes that influence vibration behaviour are also responsible for higher NFY. This leads to more rigid composites that resonate at elevated NFY in comparison to neat epoxy and composites with insufficient filler content [50]. Further addition of filler results in a decrease in NFY due to filler agglomeration within the matrix. This agglomeration increases the composite's mass and reduces its stiffness, as natural frequency is directly proportional to stiffness and inversely proportional to mass [51].

3.7. Thermogravimetric analysis

The TGA analysis was performed on PPFEC to assess thermal stability, a critical factor in polymer materials that determines the restrictions of the composite in production and applications. Fig. 8a illustrates the relationship between temperature and weight loss for PPFEC, reveals a four-stages degradation mechanism. The stage 1 is attributed to the moisture evaporation with weight loss increasing from 0.83 % (for neat epoxy) to 2.6 % (for composites with 20 wt. % of PPF) due to the existence of moisture in PPF. The stage 2 corresponds to the degradation of low-molecular-weight volatiles and hemicellulose (220–315 °C degradation temperature), leading to the moderate weight loss ranges from 2.35 to 2.98 wt. %, indicating the minimum degradation of hemicellulose present in the PPF. A maximum degradation is observed in the stage 3 for to all the composites irrespective of reinforcement content, and weight loss ranges from 77.54 %–80.51 %. These losses collectively attribute to the reinforcement constituents (hemicellulose, cellulose, partial lignin) and polymer which initiates degradation above 300 °C. Specifically, the weight loss at this region is relatively identical for composites loaded with 10 wt. % (75.34 %), and 15 wt. % (75.44 %) of PPF. The cellulosic content present in the fillers plays a key role in enhancing the structural integrity of the composites. At this stage, these cellulosic components begin to deteriorate, thereby delaying polymer degradation by absorbing significant amount ofthermal energy prior to their breakdown [52]. Char development and gradual lignin breakdown occur in Stage 4 (300–600 °C). In addition, residual char content ranging from 5.6 % to 10.68 % was obtained across different samples. Notably, composites containing 10 wt. % and 15 wt. % PPF exhibited improved char retention, attributed to enhanced

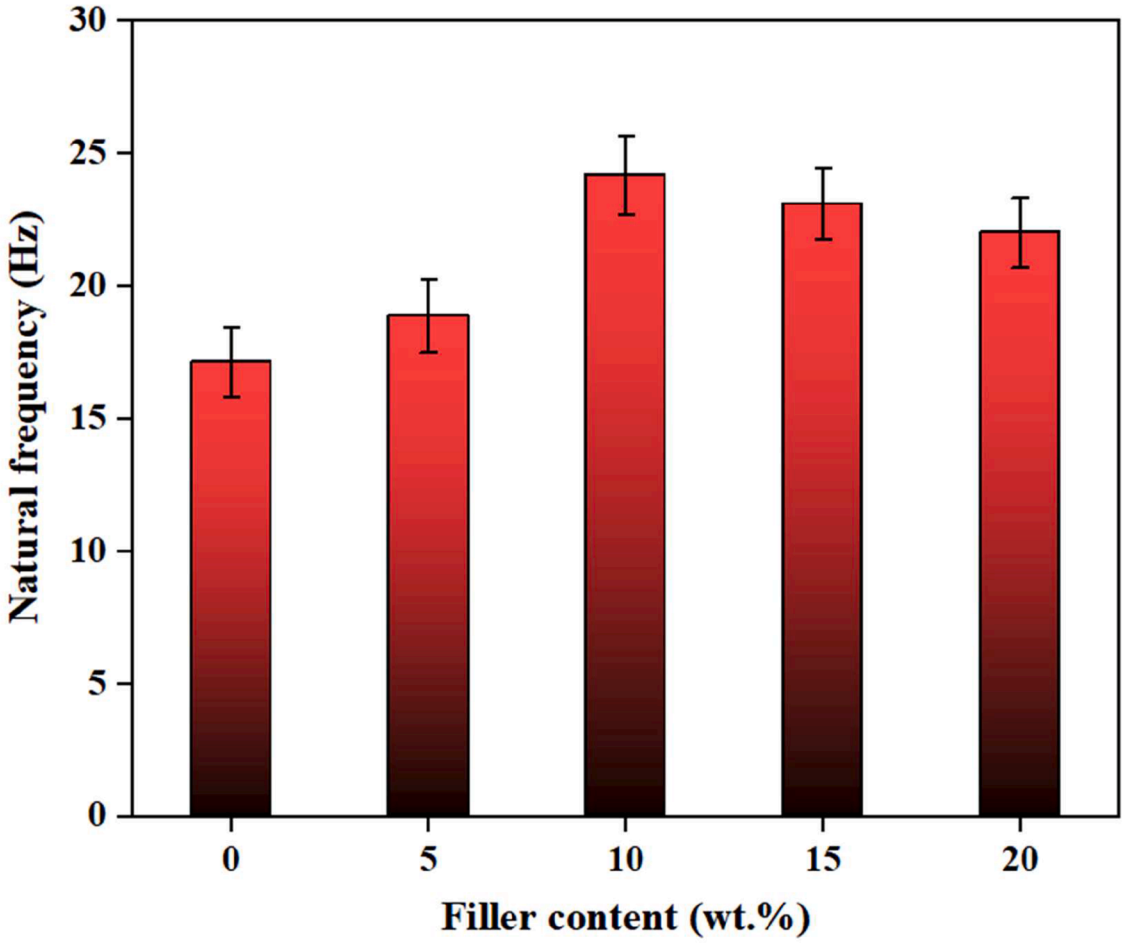

Fig. 7. Free vibration characteristics of PPFEC.

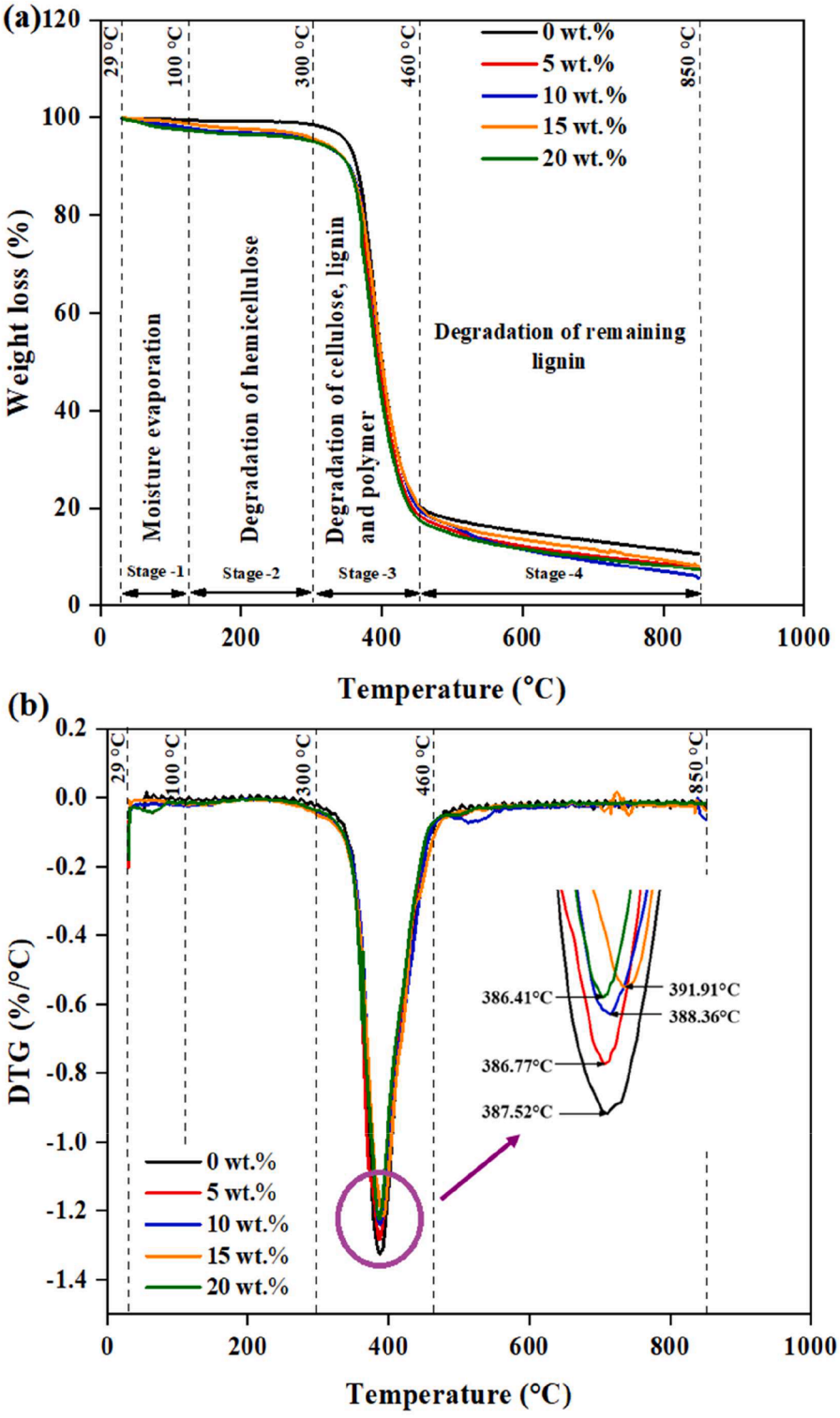

Fig. 8. Thermal behaviour of PPFEC: (a) TGA curve, and (b) DTG curve.

polymer–biomass interactions. In contrast, a higher particle loading of 20 wt. % led to reduced residue formation, suggesting increased volatile release and more complete combustion [53]. Furthermore, the neat polymer retains a higher residual char content (10.68 %) than PPF reinforced composites due to differences in thermal degradation behaviour, as polymer matrices, particularly thermosets like epoxy or phenolic resins, exhibit higher char yield due to their inherently cross-linked structure, which resists complete thermal decomposition [28].

The Derivative Thermogravimetric (DTG) analysis highlights the thermal degradation behaviour of PPFEC, showing shifts in peak degradation temperatures with the introduction of PPF, indicating its impact on thermal stability (Fig. 8b). A reasonably stable thermal profile is shown by the neat epoxy with peak breakdown temperature of 387.52 °C. While adding PPF, the corresponding peak represents the varied degradation temperatures of 386.77 °C for 5 wt. %, 388.36 °C for 10 wt.

%, 391.9 °C for 15 wt. %, and 386.41 °C for 20 wt. %. These variations indicate a change in the degradation process, due to the formation of a protective char layer that slows down decomposition, enhancing the composite's thermal stability.

3.8. DSC

The DSC analysis of the PPFECs indicates a notable shift in thermal behavior, with the plain epoxy displaying an endothermic peak at 19.55 mW, whereas the composites presented exothermic peaks (Fig. 9). The presence of an endothermic peak in the neat epoxy implies an energy-absorbing phase shift, which is most likely induced by polymer relaxation and this is due to amorphous character of the polymer [54]. The PPF-reinforced composites exhibit exothermic peaks ranging from 20.81 mW to 24.22 mW within the temperature range of 50–80 °C. The formation to exothermic peaks indicates an energy-releasing mechanism, which can be attributed to crosslinking processes and post-curing reaction. Furthermore, the biomass-based particles act as nucleation sites that allows polymer chains to align and to reorganise structurally, hence improving heat transfer [55]. The elevated exothermic peak intensities recorded in the 5 wt. % (24.22 mW) and 10 wt. % (23.64 mW) reinforced composites indicate strong polymer-filler interactions, signifying improved structural integrity. As the filler loading increases, the heat flow gradually dropped at 15 wt. % (22.23 mW) and 20 wt. % (20.81 mW) reinforcement loaded PPFEC. This downward trend implies that even though filler contributes to thermal resistance, excessive filler loading may lead to agglomeration and a reduced effective surface area, as well as weak interfacial bonding, thereby reducing the heat distribution in addition to overall stability [56] . Also, exothermic degradation peaks become broader as well as less intense, pointing to a shift from sharp energy absorption to more distributed energy release. In conclusion, such observations suggest that 5 wt. % PPF particle reinforcement provides optimum enhancement in thermal behaviour through promotion of effective filler content that restricts the free movement of polymer.

3.9. Water uptake behaviour

The water absorption behaviour of PPFEC with different filler content is depicted in the Fig. 10a. It can be noted that the water uptake by the composites augmented with the rise in PPF content. Specifically, the water absorption potential of PPFEC ranges from 14.96 % to 18.91 %, corresponding to the particle content range of 5 wt. % to 20 wt. %. The increasing pattern can be ascribed to the hydrophilic characteristics of the PPF, as the cellulose component containing hydroxyl groups (OH) affects the composite's water absorption. Furthermore, higher particle concentration reduces stiffness due to agglomeration, resulting in crack development that retains water, and also an increase in particle composition enhances the surface area of the filler exposed to water [57]. The water uptake is noted to be drastic during the initial period and attains a saturation point approximately around 64 h. The saturation point of the composites and corresponding water contact angle is displayed in Fig. 10b The water contact angle of the composite decreases with increasing PPF quantity. Specifically, the contact angle is 92.5° for the 5 wt. % PPF reinforced composite, which reduces to 85.3° at 10 wt. %, 78.4° at 15 wt. %, and further to 74.7° at 20 wt. %. This trend indicates enhanced surface hydrophilicity with increasing particle loading. The reduction in contact angle can be credited to increased surface roughness and the presence of microcracks, which promote water absorption and thereby lower contact angle is obtained [58].

The study of water absorption has been broadened to include the diffusion mechanism and kinetics of the PPFEC, applying Fick's law. There are three designated methods for transporting water in polymer composites: (i) Fickian diffusion, (ii) relaxation regulated, and (iii) pseudo-Fickian or anomalous diffusion. The parameter n governs the PPFEC diffusion process. Where $n = 0.5$ for Fickian diffusion; $0.5 \langle n < 1$ for Pseudo-Fickian diffusion; and $n \rangle 1.0$ for relaxation control [59].

To investigate the kinetics of water absorption, the experimental data were fitted to the sorption curves (Fig. 10c), as illustrated by the Eq. (5).

$$log\left(\frac{M_t}{M_{sat}}\right) = log\ (k)\ + n\ log\ (t) \tag{5}$$

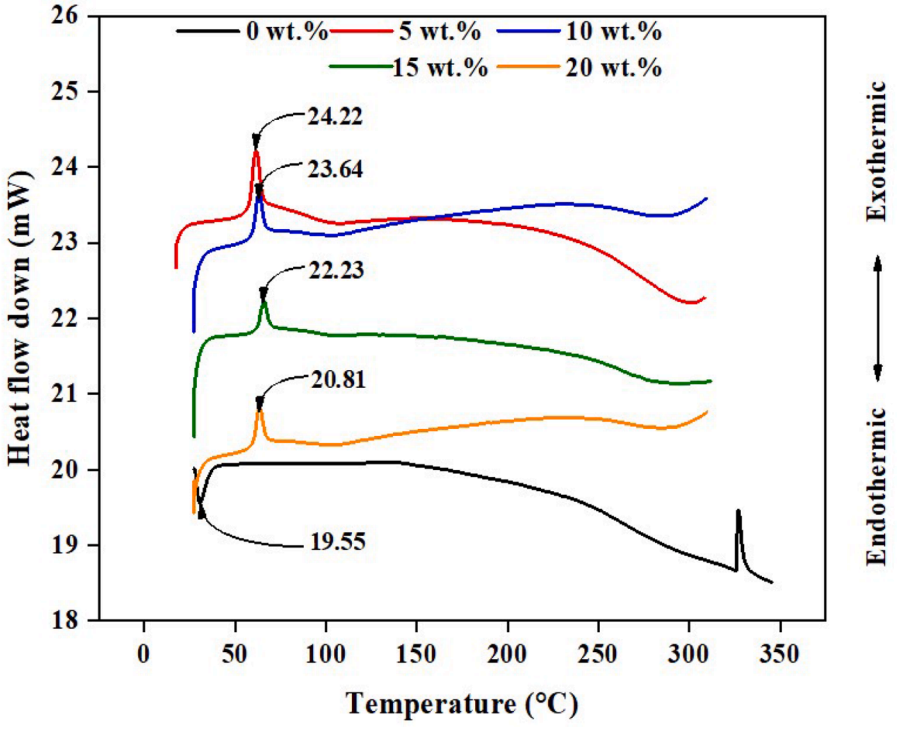

Fig. 9. DSC curve of PPFEC.

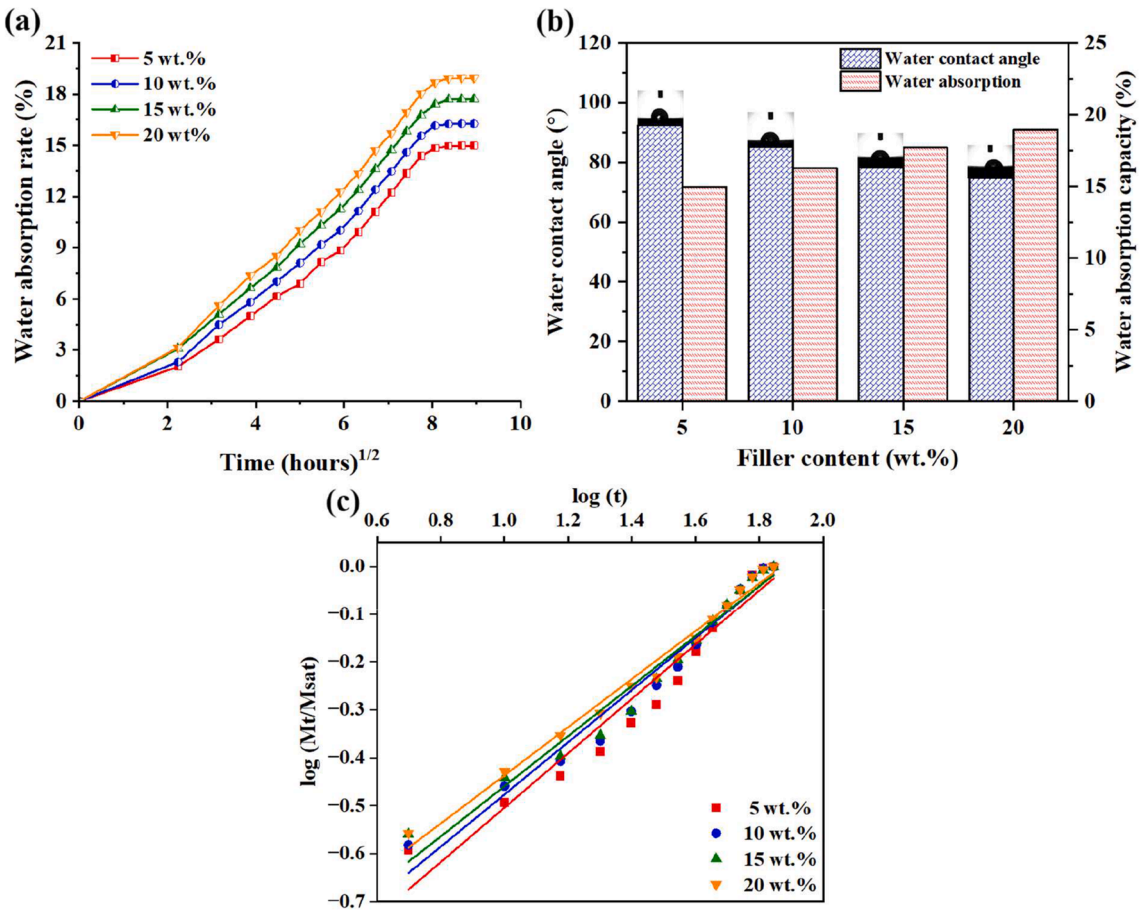

Fig. 10. Water uptake behaviour of PPFEC: (a) water uptake with time, (b) saturation point and contact angle, and (c) curve fitting.

where, M_t represents the water uptake at a given immersion time t, M_{sat} denotes the water uptake at saturation, n is the slope of the logarithmic plot of M_t/M_{sat}, k is the intercept of the logarithmic plot of M_t/M_{sat}.

In the current study, all PPFEC formulations exhibited 'n' values ranging from 0.5 to 0.56, indicating that the composites followed Fickian diffusion. Additionally, all formulations showed R^2 values close to 1, demonstrating a good fit of the model to the experimental data.

The diffusion coefficient (D), is a material-specific constant that quantifies the rate of moisture diffusion within the composite. This can be calculated using the Eq. (6) [60].

$$D = \pi \left(\frac{h}{4M_{sat}}\right)^2 \left(\frac{M_b - M_a}{\sqrt{T_b} - \sqrt{T_a}}\right)^2 \quad (6)$$

where, T_a and T_b represent selected square root of time points at linear portion of curve, and M_a and M_b denote the % of moisture uptake at T_a and T_b.

The absorption coefficient (S) is another crucial element in the kinetics of water absorption behaviour, which quantifies the rate and extent of water uptake by a material when it is exposed to moisture over time. The value of 'S' can be computed by using the Eq. (7) [61].

$$S = \frac{W_{sat}}{W_s} \quad (7)$$

where, W_s indicate the mass of the sample, and W_{sat} represent the amount of solvent absorbed at equilibrium swelling.

Also, the permeability coefficients (P) were determined by evaluating the net product of diffusion and absorption, as described by the following relation (8) [61].

$$P = D \times S \quad (8)$$

Table 5 illustrates the kinetics and transport coefficients of PPFEC. The D value of the composites notably increases from 3.08×10^{-10} m^2/min to 8.88×10^{-10} m^2/min, as filler content varied from 5 wt. % to 20 wt. %. This indicates increased mobility of water molecules through the PPFEC, probably due to increased micro voids and less resistance path created by the filler matrix interface. Similarly, the S value also increased from 0.15 to 0.19 g/g, reflecting the improved affinity of the composite towards water uptake with filler content. This behaviour represents the hydrophilic nature of the PPF, which promotes interaction with water. Since P depends on D and S, it also exhibits an increase in value from 0.46×10^{-10} to approximately 1.69×10^{-10} m^2/min. This demonstrates that, the water not only enters into the material more readily, but also penetrates much more easily at higher filler loadings.

3.10. Morphological analysis

The SEM images of the fractured surface of PPFEC, shown in Fig. 11,

Table 5
Kinetics and transport coefficients of PPFEC.

Filler wt. %	W_{sat} %	n	k	Diffusion coefficient 10^{-10} (D) (m^2/min)	Absorption coefficient (S) (g/g)	Permeability coefficient 10^{-10} (P) (m^2/min)
5	14.98	0.56	0.08504	3.08	0.15	0.46
10	16.27	0.54	0.09548	5.79	0.16	0.92
15	17.71	0.52	0.10436	7.22	0.18	1.42
20	18.94	0.50	0.11538	8.88	0.19	1.69

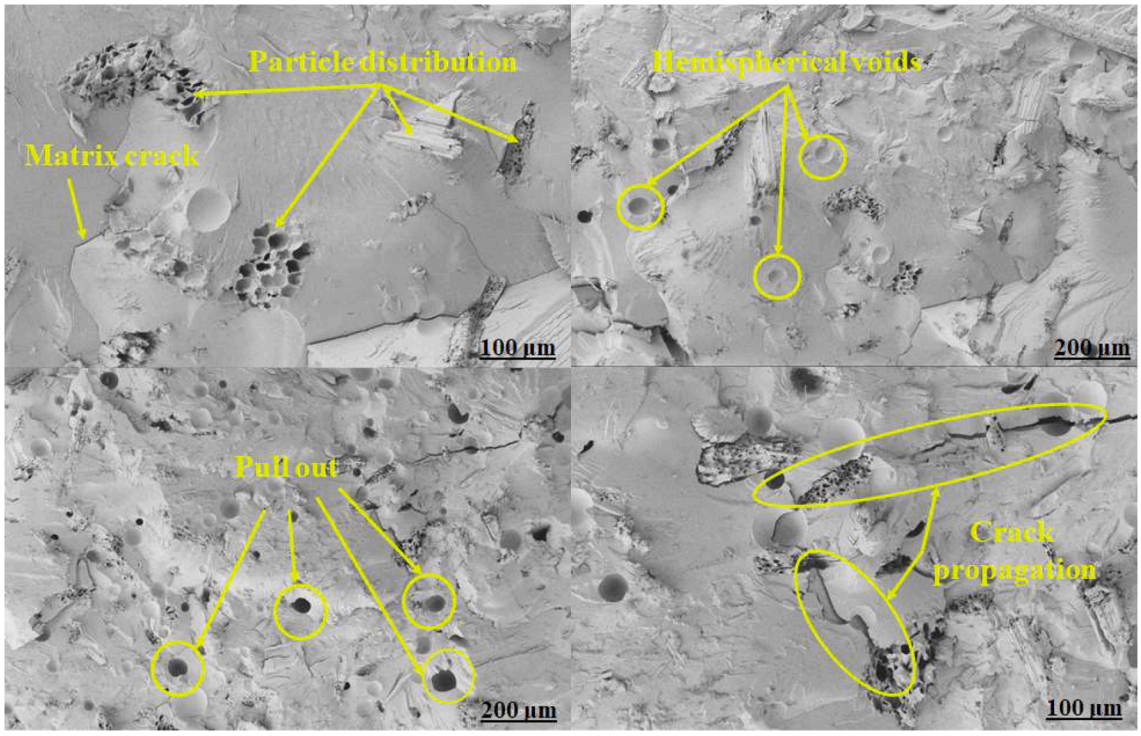

Fig. 11. SEM micrographs of PPFEC.

provide insights into the failure mechanisms, including fiber pull-out, voids, particle dispersion, and crack propagation. The uniform distribution of PPF observed in Fig. 11a facilitates effective stress transfer between the composite components, thereby enhancing the overall properties, as evidenced by the experimental results of the current study. The presence of voids and pull-outs noted in Fig. 11b-11c are the sign of poor adhesion between the PPF and the polymer matrix, which attributes to the trapped air, improper mixing, and insufficient matrix for wetting the filler during fabrication [62]. When mechanical load is applied, the existence of voids causes stress to build up, which initiates fractures and ultimately results in the complete failure of the composites [63]. Moreover, during the pull-out process, frictional and residual clamping stresses develop at the filler–matrix interface. These localized stresses contribute to elevated stress concentrations as the filler slips or debonds, serving as potential sites for stress accumulation leading to damage of the composites. From the Fig. 11d, it is clear that the propagation of crack starts from high stress concentration areas, suggests a mixed-mode of failure that includes matrix cracking and interfacial debonding. The presence of these failure mechanisms highlights the need of strong interfacial adhesion and uniform filler dispersion in reducing mechanical defects and increasing composite durability.

4. Conclusions

In the present study, polymer composites were successfully fabricated using Phoenix sp. petiole particles and an epoxy matrix through the compression moulding method. This research utilizes *Phoenix* sp. petiole particles as filler materials in polymer composites and to investigate their various properties. The following are the main conclusions drawn from this investigation - the incorporation of 10 wt. % of PPF increased tensile, flexural, and impact strengths to 41.27 %, 18.94 %, and 105.38 %, respectively compared to neat epoxy, due to uniform dispersion of PPF, better stress distribution, and enhanced stiffness of the composites. A notable improvement in hardness from 64 to 83 (Shore D) was observed with the incorporation of 10 wt. % PPF, confirming the role of effective filler–matrix bonding in enhancing mechanical properties. The natural frequency of PPFEC increases with filler content, reaching a maximum of 24.16 Hz at 10 % filler loading. However, excessive filler content leads to a reduction in both natural frequency and stiffness. Composites with finely powdered PPF exhibit improved free vibration characteristics. The TGA thermogram indicates that PPF enhanced the heat stability of the epoxy polymer by preventing early degradation, weight loss, and the evaporation of volatile components. The water absorption capacity of PPFECs increases with higher particle content, leading to greater water retention. This is attributed to enhanced surface hydrophilicity at higher filler concentrations, which promotes microfracture formation and further water uptake. The morphological analysis revealed failure mechanisms such as fiber pull-out, voids, and crack propagation, primarily attributed to poor adhesion between the PPF and the polymer matrix, weak interfacial bonding, and mixed-mode failure. These findings suggest that the material may be suitable for lightweight applications in areas such as automotive, aerospace, and structural components. Future studies will focus on improving the compatibility between the PPF and the epoxy matrix through various chemical modifications of the fillers, as well as by incorporating nanoparticles as secondary reinforcements.

Data availability

Data will be made available on request.

CRediT authorship contribution statement

G. Rajeshkumar: Writing – original draft, Methodology, Investigation, Conceptualization. **A. Poovarasan:** Writing – review & editing, Visualization, Validation, Formal analysis, Data curation. **S.V. Naren Prasaadh:** Writing – original draft, Software, Resources, Project administration, Methodology. **M.R. Sanjay:** Writing – review & editing, Validation, Methodology, Conceptualization. **Suchart Siengchin:** Writing – original draft, Validation, Supervision, Investigation.

Declaration of competing interest

The authors declare no competing interests related to this research. The processing of fillers, composite fabrication, testing, and manuscript preparation were conducted without any external funding or financial influence.

Acknowledgements

The authors gratefully acknowledge the support provided by the National Science, Research and Innovation Fund (NSRF) (Fundamental Fund 2026) and King Mongkut's University of Technology North Bangkok, Bangkok 10800, Thailand (Project No.: KMUTNB-FF-69-A-04).

References

[1] N. Singh, O.A. Ogunseitan, M.H. Wong, Y. Tang, Sustainable materials alternative to petrochemical plastics pollution: a review analysis, Sustain. Horiz. 2 (2022), https://doi.org/10.1016/j.horiz.2022.100016.
[2] M.I. Howlader, M.I. Mehedi, M.M. Alam, A.Z.M. Mofasser, N.I Sayed, M.A. Alim, M.A. Assiri, R. Mia, Mechanical and morphological analysis of natural fiber-reinforced epoxy and polyester hybrid composites, Results. Eng. 26 (2025) 105010, https://doi.org/10.1016/j.rineng.2025.105010.
[3] P. Shrivastava, M. Stafford Smith, K. O'Brien, L. Zsolnai, Transforming sustainability science to generate positive social and environmental change globally, One Earth. 2 (2020) 329–340, https://doi.org/10.1016/j.oneear.2020.04.010.
[4] K. K, M. kumar G, S.R. M, G. Tuteja, P. Das, R. Mishra, K.P. K, Exploring the antibacterial, mechanical and thermal properties of calabash fiber reinforced epoxy composite with natural fillers, Results. Eng. 25 (2025), https://doi.org/10.1016/j.rineng.2025.104113.
[5] S. Raza, J. Zhang, I. Ali, X. Li, C. Liu, Recent trends in the development of biomass-based polymers from renewable resources and their environmental applications, J. Taiwan. Inst. Chem. Eng. 115 (2020) 293–303, https://doi.org/10.1016/j.jtice.2020.10.013.
[6] O.O. Oloyede, S. Lignou, Sustainable paper-based packaging: a consumer's perspective, Foods. 10 (2021), https://doi.org/10.3390/foods10051035.
[7] L.G.L.M. Edirisinghe, A.A.P. de Alwis, M. Wijayasundara, Sustainable circular practices in the textile product life cycle: a comprehensive approach to environmental impact mitigation, Environ. Chall. 16 (2024) 100985, https://doi.org/10.1016/j.envc.2024.100985.
[8] S.K. Raju, S. Natesan, A.H. Alharbi, S. Kannan, D.S. Khafaga, M. Periyasamy, M. M. Eid, E.S.M. El-Kenawy, AHP VIKOR framework for selecting wind turbine materials with a focus on corrosion and efficiency, Sci. Rep. 14 (2024) 24071, https://doi.org/10.1038/s41598-024-72761-w.
[9] A.K. Awasthi, V.R.S. Cheela, I. D'Adamo, E. Iacovidou, M.R. Islam, M. Johnson, T. R. Miller, K. Parajuly, A. Parchomenko, L. Radhakrishan, M. Zhao, C. Zhang, J. Li, Zero waste approach towards a sustainable waste management, Resour. Environ. Sustain. 3 (2021) 100014, https://doi.org/10.1016/j.resenv.2021.100014.
[10] A. Karimah, M.R. Ridho, S.S. Munawar, D.S. Adi, R.D. Ismadi, B. Subiyanto, W. Fatriasari, A. Fudholi, A review on natural fibers for development of eco-friendly bio-composite: characteristics, and utilizations, J. Mater. Res. Technol. 13 (2021) 2442–2458, https://doi.org/10.1016/j.jmrt.2021.06.014.
[11] J. Iyyadurai, V.C.S. Gandhi, I. Suyambulingam, G. Rajeshkumar, Sustainable development of Cissus quadrangularis stem Fiber/epoxy composite on abrasive wear rate, J. Nat. Fibers 19 (2022) 9283–9295, https://doi.org/10.1080/15440478.2021.1982819.
[12] N.S. R, S.M.K. Thiagamani, S. P, S. M, S.N. Boyina Yagna, E.K. Hossein, M. M, S. Mavinkere Rangappa, S. Siengchin, Isolation and characterization of agro-waste biomass sapodilla seeds as reinforcement in potential polymer composite applications, Heliyon 9 (2023) e17760, https://doi.org/10.1016/j.heliyon.2023.e17760.
[13] R. Shyam Narain, Recent advancements and challenges in green material technology: preparing today for nourishing tomorrow, Mater. Today Proc. (2023), https://doi.org/10.1016/j.matpr.2023.02.218.
[14] X. Xing, N.S. Alharbi, X. Ren, C. Chen, Journal of Environmental Chemical Engineering A comprehensive review on emerging natural and tailored materials for chromium-contaminated water treatment and environmental remediation, J. Environ. Chem. Eng. 10 (2022) 107325, https://doi.org/10.1016/j.jece.2022.107325.
[15] Y. Cai, Z. Liu, K. Gong, Y. Zhang, The effect of reinforcement particle size on the mechanical and fracture properties of glass matrix composites, Heliyon. 9 (2023) e21895, https://doi.org/10.1016/j.heliyon.2023.e21895.
[16] P. RaviKumar, G. Rajeshkumar, J. Prakash Maran, N.A. Al-Dhabi, P. Karuppiah, Evaluation of mechanical and water absorption behaviors of jute/carbon Fiber reinforced polyester hybrid composites, J. Nat. Fibers 19 (2022) 6521–6533, https://doi.org/10.1080/15440478.2021.1924339.
[17] N. Karthi, K. Kumaresan, G. Rajeshkumar, S. Gokulkumar, S. Sathish, Tribological and thermo-mechanical performance of chemically modified Musa Acuminata /corchorus capsularis reinforced hybrid composites, J. Nat. Fibers 19 (2022) 4640–4653, https://doi.org/10.1080/15440478.2020.1870614.
[18] N. Nagaraj, S. Balasubramaniam, V. Venkataraman, R. Manickam, R. Nagarajan, I. S. Oluwarotimi, Effect of cellulosic filler loading on mechanical and thermal properties of date palm seed/vinyl ester composites, Int. J. Biol. Macromol. 147 (2020) 53–66, https://doi.org/10.1016/j.ijbiomac.2019.11.247.
[19] K.J. Nagarajan, A.N. Balaji, K.S. Basha, N.R. Ramanujam, R.A. Kumar, Effect of agro waste α-cellulosic micro filler on mechanical and thermal behavior of epoxy composites, Int. J. Biol. Macromol. 152 (2020) 327–339, https://doi.org/10.1016/j.ijbiomac.2020.02.255.
[20] N. Sienkiewicz, M. Dominic, J. Parameswaranpillai, Natural fillers as potential modifying agents for epoxy composition: a review, Polymers 14 (2022) 1–17, https://doi.org/10.3390/polym14020265.
[21] G. Rajeshkumar, V. Hariharan, Characterization of Phoenix sp . natural fiber as potential reinforcement of polymer composites, (2016). https://doi.org/10.1177/1528083715591581.
[22] M.G. Ranjithkumar, P. Chandrasekaran, G. Rajeshkumar, Characterization of sustainable natural fiber reinforced geopolymer composites, Polym. Compos. 43 (2022) 3691–3698, https://doi.org/10.1002/pc.26646.
[23] G. Rajeshkumar, Mechanical and free vibration properties of Phoenix sp. fiber reinforced epoxy composites: influence of sodium bicarbonate treatment, Polym. Compos. 42 (2021) 6362–6369, https://doi.org/10.1002/pc.26303.
[24] M.W. Tham, M.N. Fazita, H.A. Khalil, N.Z. Mahmud Zuhudi, M. Jaafar, S. Rizal, M. M. Haafiz, Tensile properties prediction of natural fibre composites using rule of mixtures: a review, J. Reinf. Plast. Compos. 38 (2019) 211–248, https://doi.org/10.1177/0731684418813650.
[25] A. Atmakuri, A. Palevicius, A. Vilkauskas, G. Janusas, Numerical and experimental analysis of mechanical properties of natural-Fiber-reinforced hybrid polymer composites and the effect on matrix material, Polymers 14 (2022) 2612, https://doi.org/10.3390/polym14132612.
[26] S. Greenough, M.J. Dumont, S. Prasher, The physicochemical properties of biochar and its applicability as a filler in rubber composites: a review, Mater. Today Commun. 29 (2021), https://doi.org/10.1016/j.mtcomm.2021.102912.
[27] L. Hu, X. Fang, M. Du, F. Luo, S. Guo, Hemicellulose-based polymers processing and application, Am. J. Plant Sci. 11 (2020) 2066–2079, https://doi.org/10.4236/ajps.2020.1112146.
[28] G. Zhou, E. Mikinka, J. Golding, X. Bao, W. Sun, A. Ashby, Investigation of thermal degradation and decomposition of both pristine and damaged carbon/epoxy samples with thermal history, Compos. B Eng. 201 (2020) 108382, https://doi.org/10.1016/j.compositesb.2020.108382.
[29] J.C. Markwart, A. Battig, M.M. Velencoso, D. Pollok, B. Schartel, F.R. Wurm, Aromatic vs. aliphatic hyperbranched polyphosphoesters as flame retardants in epoxy resins, Molecules 24 (2019) 1–15, https://doi.org/10.3390/molecules24213901.
[30] G. Rajeshkumar, V. Hariharan, T.P. Sathishkumar, Characterization of Phoenix sp. natural fiber as potential reinforcement of polymer composites, J. Ind. Text. 46 (2016) 667–683, https://doi.org/10.1177/1528083715591581.
[31] T. Durak, J. Depciuch, Effect of plant sample preparation and measuring methods on ATR-FTIR spectra results, Environ. Exp. Bot. 169 (2020) 103915, https://doi.org/10.1016/j.envexpbot.2019.103915.
[32] S. Zhang, X. Wang, J. Yang, H. Chen, X. Jiang, Micromechanical interlocking structure at the filler/resin interface for dental composites: a review, Int. J. Oral Sci. 15 (2023), https://doi.org/10.1038/s41368-023-00226-3.
[33] G.E. Rani, R. Murugeswari, S. Siengchin, N. Rajini, M.A. Kumar, Quantitative assessment of particle dispersion in polymeric composites and its effect on mechanical properties, J. Mater. Res. Technol. 19 (2022) 1836–1845, https://doi.org/10.1016/j.jmrt.2022.05.147.
[34] P. Pitch, C. Structure, Y. Mamunya, A. Misiura, M. Godzierz, S. Pusz, U. Szeluga, Polymer composites with carbon fillers based on coal pitch, (2024).
[35] H.T.N. Kuan, M.Y. Tan, Y. Shen, M.Y. Yahya, Mechanical properties of particulate organic natural filler-reinforced polymer composite: a review, Compos. Adv. Mater. 30 (2021) 263498332110075, https://doi.org/10.1177/26349833211007502.
[36] I.O. Oladele, A.S. Taiwo, L.J. Bello, S.O. Balogun, L. Senzeni Sipho, S.O. Adelani, Fabrication of animal shell and sugarcane bagasse particulate hybrid reinforced epoxy composites for structural applications, Polym. Polym. Compos. 32 (2024) 1–12, https://doi.org/10.1177/09673911231202183.
[37] I. Khan, N. Kumar, M. Choudhary, S. Kumar, T. Singh, Mechanical and dynamic mechanical behavior of 3D printed waste slate particles filled acrylonitrile butadiene styrene composites, Arab, J. Chem. 17 (2024) 105559, https://doi.org/10.1016/j.arabjc.2023.105559.
[38] M. Megahed, A. Fathy, D. Morsy, F. Shehata, Mechanical performance of glass/epoxy composites enhanced by micro- and nanosized aluminum particles, J. Ind. Text. 51 (2021) 68–92, https://doi.org/10.1177/1528083719874479.
[39] J.M. Aldabib, Z.A.M. Ishak, Effect of hydroxyapatite filler concentration on mechanical properties of poly (methyl methacrylate) denture base, SN. Appl. Sci. 2 (2020) 1–14, https://doi.org/10.1007/s42452-020-2546-1.
[40] R.O. Akaluzia, F.O. Edoziuno, A.A. Adediran, B.U. Odoni, S. Edibo, T.M. A. Olayanju, Evaluation of the effect of reinforcement particle sizes on the impact and hardness properties of hardwood charcoal particulate-polyester resin composites, Mater. Today Proc. 38 (2021) 570–577, https://doi.org/10.1016/j.matpr.2020.02.980.
[41] V. Mohanavel, K. Rajan, S. Suresh Kumar, G. Vijayan, M.S. Vijayanand, Study on mechanical properties of graphite particulates reinforced aluminium matrix composite fabricated by stir casting technique, Mater. Today Proc. 5 (2018) 2945–2950, https://doi.org/10.1016/j.matpr.2018.01.090.

[42] A.P. Irawan, J.P. Siregar, T. Cionita, D.F. Fitriyana, A. Alias, R. Rusiyanto, J. Jaafar, P. Prayitno, R. Ismail, A.P. Bayuseno, A.A. Janvekar, Elaeocarpus ganitrus (rudraksha) seeds as a potential sustainable reinforcement for polymer matrix composites, Polym. Compos. 45 (2024) 4662–4679, https://doi.org/10.1002/pc.28088.

[43] O. Shakuntala, G. Raghavendra, A.S. Kumar, Effect of filler loading on mechanical and tribological properties of wood Apple shell reinforced epoxy composite, Adv. Mater. Sci. Eng. 2014 (2014) 538651, https://doi.org/10.1155/2014/538651.

[44] K.K. Basumatary, Investigation into mechanical properties of Ipomoea carnea reinforced epoxy composite ISSN-2249-8559 original article Investigation into mechanical properties of Ipomoea carnea reinforced epoxy composite, 3 (2014) 11–15.

[45] S. Mohanty, S. Shukla, D. Senapati, G. Sahoo, D. Sahoo, S.P. Mohanty, Tamarind seed powder as filler in polypropylene and its impact on the mechanical and biodegradability of the composites, Int. Polym. Process. 40 (2025) 34–42, https://doi.org/10.1515/ipp-2024-0063.

[46] G. Raghavendra, S. Ojha, S. Kumar Acharya, P. Kumar, Fabrication and study of mechanical properties of orange PEEL reinforced polymer composite, Casp. J. Appl. Sci. Res. 1 (2012) 190–194.

[47] B. Stalin, N. Nagaprasad, V. Vignesh, M. Ravichandran, Evaluation of mechanical and thermal properties of tamarind seed filler reinforced vinyl ester composites, J. Vinyl. Addit. Technol. 25 (2019) E114–E128, https://doi.org/10.1002/vnl.21701.

[48] B. Stalin, N. Nagaprasad, V. Vignesh, M. Ravichandran, N. Rajini, S.O. Ismail, F. Mohammad, Evaluation of mechanical, thermal and water absorption behaviors of Polyalthia longifolia seed reinforced vinyl ester composites, Carbohydr. Polym. 248 (2020), https://doi.org/10.1016/j.carbpol.2020.116748.

[49] K. Kushwanth Theja, G. Bharathiraja, V. Sakthi Murugan, A. Muniappan, Evaluation of mechanical properties of tea dust filler reinforced polymer composite, Mater. Today Proc. 80 (2023) 3208–3211, https://doi.org/10.1016/j.matpr.2021.07.213.

[50] L. K S, S.M. D, Y. H L, S. I S, H. Nikam, C.K.R. K L, Evaluation of mechanical, acoustic and vibration characteristics of calamus rotang based hybrid natural fiber composites, Results. Eng. 25 (2025) 104475, https://doi.org/10.1016/j.rineng.2025.104475.

[51] G. Rajeshkumar, M.R. Sanjay, S. Siengchin, V. Hariharan, Influence of sodium bicarbonate treatment on the free vibration characteristics of Phoenix sp. fiber loaded polyester composites, Mater, Today Proc. 52 (2021) 2400–2403, https://doi.org/10.1016/j.matpr.2021.10.414.

[52] A. Quitadamo, V. Massardier, V. Iovine, A. Belhadj, R. Bayard, M. Valente, Effect of cellulosicwaste derived filler on the biodegradation and thermal properties of HDPE and PLA composites, Processes 7 (2019), https://doi.org/10.3390/pr7100647.

[53] H.L. Ornaghi, F.G. Ornaghi, R.M. Neves, F. Monticeli, O. Bianchi, Mechanisms involved in thermal degradation of lignocellulosic fibers: a survey based on chemical composition, Cellulose 27 (2020) 4949–4961, https://doi.org/10.1007/s10570-020-03132-7.

[54] B.Z. Marchi, P.H.P.M. da Silveira, W.B.A. Bezerra, L.F.C. Nascimento, F.P.D. Lopes, V.S. Candido, A.C.R. da Silva, S.N. Monteiro, Ballistic performance, thermal and chemical characterization of Ubim Fiber (Geonoma baculifera) reinforced epoxy matrix composites, Polymers. (Basel) (2023) 15, https://doi.org/10.3390/polym15153220.

[55] M. Bartoli, R. Arrigo, G. Malucelli, A. Tagliaferro, D. Duraccio, Recent advances in biochar polymer composites, Polymers 14 (2022) 1–30, https://doi.org/10.3390/polym14122506.

[56] C. Balaji Ayyanar, S. Pradeep Mohan, M. Ramesh, L. Rajeshkumar, K. Marimuthu, M. Sanjay, S. Siengchin, Effect of natural fillers as reinforcements on mechanical and thermal properties of HDPE composites, J. Thermoplast. Compos. Mater. 37 (2024) 800–819, https://doi.org/10.1177/08927057231186312.

[57] K. Yorseng, S.M. Rangappa, J. Parameswaranpillai, S. Siengchin, Influence of accelerated weathering on the mechanical, fracture morphology, thermal stability, contact angle, and water absorption properties of natural fiber fabric-based epoxy hybrid composites, Polymers 12 (2020) 1–14, https://doi.org/10.3390/polym12102254.

[58] W. Song, A. Gu, G. Liang, L. Yuan, Effect of the surface roughness on interfacial properties of carbon fibers reinforced epoxy resin composites, Appl. Surf. Sci. 257 (2011) 4069–4074, https://doi.org/10.1016/j.apsusc.2010.11.177.

[59] J.P. Manaia, A. Manaia, Interface modification, water absorption behaviour and mechanical properties of injection moulded short hemp fiber-reinforced thermoplastic composites, Polymers 13 (2021), https://doi.org/10.3390/polym13101638.

[60] G. Rajeshkumar, An experimental study on the interdependence of mercerization, moisture absorption and mechanical properties of sustainable Phoenix sp. fibre-reinforced epoxy composites, J. Ind. Text. 49 (2020) 1233–1251, https://doi.org/10.1177/1528083718811085.

[61] N.H.I. Kamaludin, H. Ismail, A. Rusli, S.S. Ting, Thermal behavior and water absorption kinetics of polylactic acid/chitosan biocomposites, Iran, Polym. J. Engl. Ed. 30 (2021) 135–147, https://doi.org/10.1007/s13726-020-00879-5.

[62] M. Mehdikhani, L. Gorbatikh, I. Verpoest, S.V. Lomov, Voids in fiber-reinforced polymer composites: a review on their formation, characteristics, and effects on mechanical performance, J. Compos. Mater. 53 (2019) 1579–1669, https://doi.org/10.1177/0021998318772152.

[63] M.M.A. Nassar, B.J. Abu Tarboush, K.I. Alzebdeh, N. Al-Hinai, T. Pervez, New synthesis routes toward improvement of natural filler/synthetic polymer interfacial crosslinking, Polymers. (Basel) 14 (2022), https://doi.org/10.3390/polym14030629.